JOURNAL OF MATERIALS SCIENCE 31 (1996) 1151–1156

Morphology and structure of $ZnCr_2O_4$ spinel crystallites

D. J. BINKS, R. W. GRIMES
Department of Materials, Imperial College of Science, Technology and Medicine, Prince Consort Road, London SW7 2BP, UK

A.L. ROHL, D.H. GAY
Davy-Faraday Laboratory, The Royal Institution of Great Britain, 21 Albemarle Street, London W1X 4BS, UK

Computer simulation techniques have been used to predict the crystal morphology of the spinel $ZnCr_2O_4$. In agreement with experiment, crystallites are predicted to be essentially octahedral with the {1 1 1} surface dominating the structure. However, surfaces for materials with the spinel structure are highly complex and stabilized only by the formation of surface defects. This leads to a large number of different possible surface structures.

1. Introduction

Our interest in $ZnCr_2O_4$ is in its applications as a gas sensor [1] and as a catalyst [2–5]. As such, knowledge of the surface structure would be most useful. Indeed, in order to understand fully how any ceramic material interacts with its environment, it is necessary to determine the atomic structure at its surface. This work is a first step in this process for $ZnCr_2O_4$ and shows, amongst other things, what a complex task this is.

Computer simulation techniques can play an important role in developing our understanding of surfaces. However, even though the accurate simulation of the bulk properties of many ionic solids is now common place, the calculation of surface structures presents a greater computational demand. A surface must be modelled as a structure which is periodic in two dimensions, that is, a slab. The thickness of the slab must be at least 4 nm in order to ensure that the top layers of ions at the end close to the free surface are subject to a realistic model for the forces emanating from the bulk. If a material is periodic, periodic boundary conditions can be implemented which usually reduce quite considerably the number of ions that must be modelled explicitly. Thus a three-dimensional periodic structure can be easier to model than one which has two-dimensional periodicity.

In addition to computational restrictions, problems remain in that we can generally only derive a model for the inter-ionic forces from the properties of a bulk lattice. In this study we negate such problems by using a multiple fitting process for potential derivation [6] as described below.

The aim of our study was to examine the low index surfaces of $ZnCr_2O_4$ in terms of their calculated attachment and surface energies and to use these data to predict the resultant crystal morphology which can then be compared with experiment. In addition, detailed atomic structure of a surface has also been predicted. Unfortunately, as recently stated by Henrich and Cox [7], there are at present no experimental studies of the surface atomic structure of spinel oxides.

In a previous theoretical study of the archetypal spinel, $MgAl_2O_4$, Davies *et al.* [8] used surface energies to predict crystallite morphology. In agreement with this study, they found that the (1 0 0) surface was dominant in the unrelaxed morphology. However, upon relaxation, our work suggests that the (1 1 1) surface becomes dominant, whilst Davies *et al.* predicted that the (1 0 0) would remain the lowest energy surface.

2. Methodology

2.1. Description of interactions between ions

Calculations were performed using the general surface code MARVIN [9]. This procedure is based upon a description of the lattice in terms of inter-ionic potentials. We consider interactions due to long-range Coulombic forces, which are summed using a variation of Ewald's method by Parry [10, 11], suitable for two-dimensional structures. Short-range forces are also modelled, by using parameterized pair potentials. The short-range terms account for the electron cloud overlap and dispersion reactions which are negligible beyond to a few lattice spacings. The Buckingham potential form was chosen to represent the short-range contribution to the interaction energy, $E(r)$, so that the total interaction between two ions i and j can be written,

$$E(r_{ij}) = \frac{q_i q_j}{r_{ij}} + A\exp(-r_{ij}/\rho) - C/r^6 \quad (1)$$

where A, ρ and C are the variable parameters, see Table I.

TABLE I Zinc chromite potential parameters

Species	A (eV)	ρ (nm)	C (eV nm^{-6})
O^{2-}–O^{2-}	9547.96	0.2192	32.0×10^6
Zn^{2+}–O^{2-}	529.7	0.3581	0.0
Cr^{3+}–O^{2-}	1204.18	0.3165	0.0

TABLE II Oxygen shell model parameters

Species	Y (e)	k (eV nm^{-2})
O^{2-}	−2.04	630

Given the existence of a free surface it is possible that ions may undergo extensive surface relaxation. As such a surface, inter-ionic separations can be very different from those in the bulk. Consequently, care must be taken to ensure that the inter-ionic potentials are valid over this extended set of inter-ionic distances.

With this in mind, the potential set used here has not been derived solely for $ZnCr_2O_4$ but for a series of oxides including the three polymorphs of zinc oxide and Cr_2O_3; consequently, the potentials are valid over a significantly wider range of inter-ionic distances. The same potential set has been used successfully in previous studies of the varistor behaviour of ZnO [12] and the redox characteristics of $ZnCr_2O_4$ [13].

Oxygen ions are treated as polarizable and described by the shell model [14]. In this, a massless shell of charge Y is allowed to move with respect to a massive core of charge X; the charge state of each ion is therefore equal to $(X + Y)$. In this study we use formal charges for all ions (e.g. O^{2-}, Zn^{2+}, Cr^{3+}). The core and shell charges are connected by an isotropic harmonic spring of force constant k, see Table II.

The shell charge and force constant were chosen in such a way that the high-frequency dielectric constant of ZnO was correctly reproduced. In line with studies of many other oxides whose cations are significantly less polarizable than oxygen, we model all cations as rigid ions [15]. Discussions of the model parameters and of the methodology generally can be found in recent reviews [16–19].

2.2. Simulating a free surface

The crystal lattice is divided into two regions; region I represents the ions close to the surface which are directly affected by the termination of the lattice, whilst region II incorporates the ions which are so far removed from the surface as to be regarded as bulk lattice ions. Consequently, only region I ions are relaxed explicitly and thus the total energy of the surface is dependent on allowing the ions in region I to relax to zero strain. In this study, a region I depth of 0.93 nm was found to be sufficient, such that any further increase had no effect on the surface relaxation.

The shape of a crystallite can be determined by two separate methods termed the growth and equilibrium morphologies. Whilst the growth morphology is based upon the energetics associated with the deposition of blocks of material upon all of the competing growth surfaces, the equilibrium morphology is simply that which reduces the total surface energy to a minimum value.

The determination of the growth morphology requires the calculation of the attachment energy, which is defined as [9] the "energy released when a further growth slice is brought from an infinite distance on to the growing crystal surface". Hence it is related to the crystal bulk energy and the growth slice energy by

$$\text{Attachment energy} = \text{bulk energy} - \text{slice energy} \tag{2}$$

In the case of a non-defective surface, the growth slice is simply a flat slab of ions; however, when defective surfaces are modelled, the growth slice must contain "troughs" and "steps" to reflect accurately the vacancy and interstitial defect species.

The equilibrium morphology is based upon the relative energies of each of the crystallite surfaces. The energy of any given surface is that required to produce that surface by splitting a bulk crystal lattice, i.e.

$$\text{surface energy} = \frac{E_{\text{surf}} - E_{\text{bulk}}}{A} \tag{3}$$

where E_{surf} is the energy of the ions at the surface, E_{bulk} is the equivalent value for ions in the bulk lattice and A is the surface area.

Any flat cut to form a surface in $ZnCr_2O_4$ produces a dipole perpendicular to the plane of that surface, i.e. a type III surface is formed [20]. The contribution of the dipole to the surface energy will increase simply as a function of the thickness of the surface slab; thus the surface energy will not converge as a function of Region I and II size. Clearly such a surface cannot exist unless it is stabilized by the removal of the dipole through the creation of surface defects, i.e. the addition of surface ions to form charged interstitial ions or the removal of lattice ions to produce a surface vacancy. Hence for each surface the initial dipole was removed by the addition of defects prior to the calculation of the relaxed surface and attachment energies.

3. Results and discussion

The morphology of a crystalline lattice is usually determined by the low index surfaces with large d spacing where

$$\frac{1}{d^2} = \frac{1}{h^2} + \frac{1}{k^2} + \frac{1}{l^2} \tag{4}$$

Thus the valid surfaces for the spinel lattice are, in order of decreasing d spacing, (1 1 1), (2 2 0), (4 0 0), (3 1 1), (3 3) 1, (4 2 2) and (5 1 1). Unfortunately, as the d spacing is reduced, the surface area is increased and the number of ions requiring explicit relaxation rapidly becomes prohibitively large. Consequently, only the first three surfaces, i.e. (1 1 1), (2 2 0) and (4 0 0) have been simulated in this work. The use of the indices (2 2 0) instead of (1 1 0) and (4 0 0) instead of (1 0 0) allows for the inherent repeat units within those

surfaces; the (1 1 0) has two repeats and the 1 0 0 possesses four. This allows direct comparison of the attachment energies.

Within any crystallographic lattice there will exist one or more different z values, assuming that z lies perpendicular to the surface, at which it is possible to "cut" the lattice in order to form a new surface. Each of these cut values will produce a surface terminated by different numbers and/or types of ions.

This number of cuts is further compounded as there is a large number of combinations of defects that can be used to stabilize any given surface cut. Take, for example, one instance where the surface requires the movement of charge equivalent to that of 14 electrons; this corresponds to the (1 1 1) surface cut at a shift of 0.0703. There is a myriad of possibilities as to how this can be achieved using the three negative defect species available, i.e. $V^{\bullet\bullet}_{Zn}$, $V^{\bullet\bullet\bullet}_{Cr}$ and $O^{\bullet\bullet}_i$. In order to perform a comprehensive study, each of these possibilities has been considered. In this way it is possible to investigate the effect of different defect species upon both the surface and attachment energies. Figs 1 and 2 show how the relative energies differ as a single cut is stabilized first by purely $V^{\bullet\bullet}_{Zn}$ defects, and at the other extreme by incorporating only $O^{\bullet\bullet}_i$ defects. We also consider all the intermediate combinations, i.e. $7V^{\bullet\bullet}_{Zn}$, $(6V^{\bullet\bullet}_{Zn} + 1O^{\bullet\bullet}_i)$, $(5V^{\bullet\bullet}_{Zn} + 2O^{\bullet\bullet}_i)$, ... $(1V^{\bullet\bullet}_{Zn} + 6O^{\bullet\bullet}_i)$, $7O^{\bullet\bullet}_i$. Of course, in the full calculations, we also considered combinations such as, $2V^{\bullet\bullet\bullet}_{Cr} + 2V^{\bullet\bullet}_{Zn} + 2O^{\bullet\bullet}_i$.

The figures illustrate two fundamental points. Firstly, the relationship between surface energy and defect type is not linear. Secondly, whilst the attachment energy is changed little by relaxation, the surface energy values are capable of being substantially reduced. Indeed, irrespective of the unrelaxed surface energy, the relaxed values are strikingly similar. Although each of these different cuts together with the different defects were considered in terms of their attachment and surface energies, only those that dominate the morphology are reported, see Tables III and IV. Nevertheless, it should be noted that the combination of cuts and surfaces resulted in our carrying out calculations for: 303 (1 1 1) surfaces; 14 (2 2 0) surfaces and 14 (4 0 0) surfaces. All relevant data and energies for these are reported elsewhere [6].

Table III shows the favoured attachment energy values for each surface. Clearly the (1 1 1) surface is the least exothermic when a further growth slice is deposited on the growing surface. Consequently, it will be the slowest growing surface and will therefore dominate both the relaxed and unrelaxed morphologies, shown in Figs 3 and 4. The effect of relaxation on the predicted morphology is important, as it serves to produce a small amount of capping of the octahedral vertices.

In contrast, the surface energies reported in Table IV show a great deal of variation between the relaxed and unrelaxed states. This is clearly reflected in the predicted morphologies shown in Figs 5 and 6 where the (4 0 0) dominated cube is transformed into a heavily capped octahedron upon relaxation.

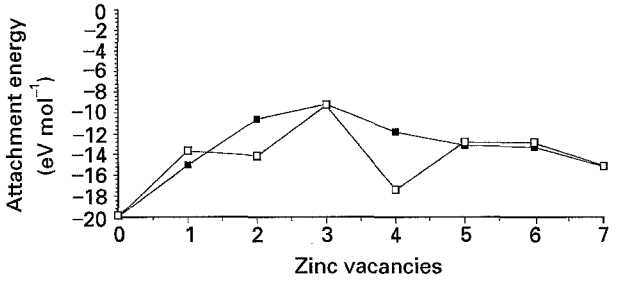

Figure 1 Relationship of the attachment energy to stabilizing defects: (■) unrelaxed, (□) relaxed.

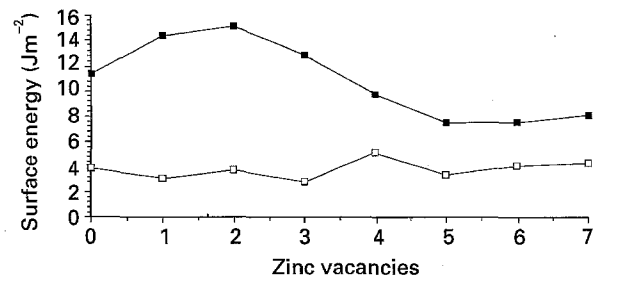

Figure 2 Relationship of the surface energy to stabilizing defects: (■) unrelaxed, (□) relaxed.

TABLE III Zinc chromite attachment energies

	Calculated attachment energies (eV mol^{-1})		
Surface	Defects	Unrelaxed	Relaxed
{1 1 1}	$4O^{\bullet\bullet}_i + 3V^{\bullet\bullet}_{Zn}$	−9.14	−8.89
{2 2 0}	$O^{\bullet\bullet}_i$	−14.97	−13.94
{4 0 0}	$Zn^{\bullet\bullet}_i$	−15.98	−14.82

TABLE IV Zinc chromite surface energies

Surface	Calculated surface energies (J m^{-2})		
	Defect	Unrelaxed	Relaxed
{1 1 1}	$6V^{\bullet\bullet}_{Zn} + 2V^{\bullet\bullet\bullet}_{Cr}$	49.25	1.78
{2 2 0}	$O^{\bullet\bullet}_i$	4.99	2.59
{4 0 0}	$Zn^{\bullet\bullet}_i$	3.49	2.04

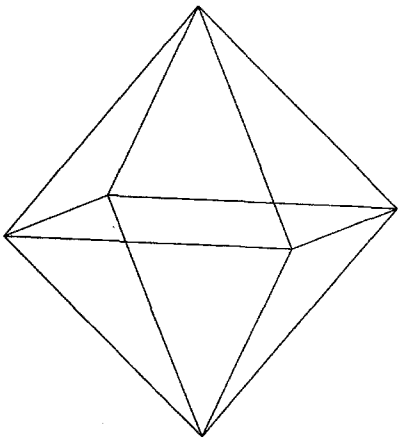

Figure 3 Predicted morphology using unrelaxed attachment energies.

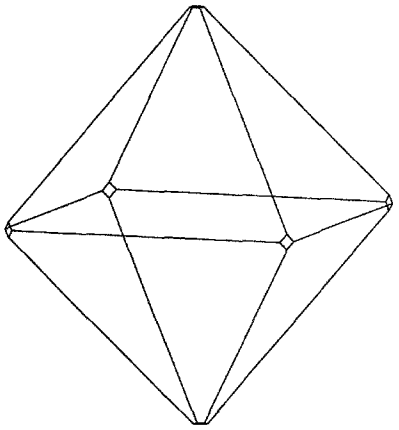

Figure 4 Predicted morphology using relaxed attachment energies.

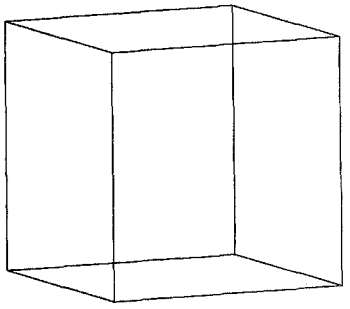

Figure 5 Predicted morphology using unrelaxed surface energies.

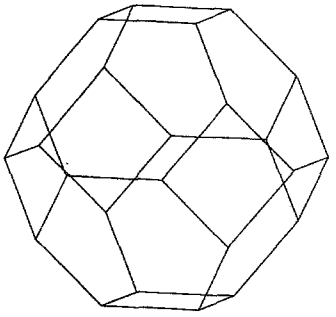

Figure 6 Predicted morphology using relaxed surface energies.

Clearly the two methods predict morphologies dominated by the (1 1 1) surface but the tiny caps predicted by the attachment energy are (2 2 0) in origin whilst the large caps predicted by the equilibrium morphology are (4 0 0) in origin.

Figs 7–10 show the atomic structure of the surfaces listed in Tables III and IV. For each surface, both a surface profile (top) and elevated view (bottom) are shown for the unrelaxed (far left) and relaxed (far right) structures. For the purposes of the diagrams alone the lattices have been truncated at a depth of 0.6 nm below the surface.

Upon relaxation, the $Zn_i^{\bullet\bullet}$ ions that stabilize the (4 0 0) surface can be seen to retract into the surface by a small amount. A similar effect is seen for (2 2 0) where the O_i'' ions again sink into the surface plane upon relaxation, though the effect appears to be less pronounced, possibly simply due to the larger size of the oxygen ion.

Figs 9 and 10 show the (1 1 1) surfaces; however, here in each case, the relaxation is much more extensive compared to that for the two previous surfaces. This, together with the large increase in the number of ions requiring explicit relaxation, serves to re-emphasize the computational demands associated with the higher index surfaces.

Given the small relaxations apparent in the (4 0 0) and (2 2 0) surface layers, it is not surprising to see that ions in the next two layers appear to occupy perfect lattice sites (compare the relaxed and unrelaxed surface profiles in Figs 7 and 8). What is significant is that for the (1 1 1) surface by the third layer down from the surface, relaxations appear to be minimal. Given the extensive surface re-arrangements one might have expected relaxation to be apparent in greater depth.

4. Conclusion

Several zinc chromite crystals have been grown experimentally [21, 22]. Careful examination of these

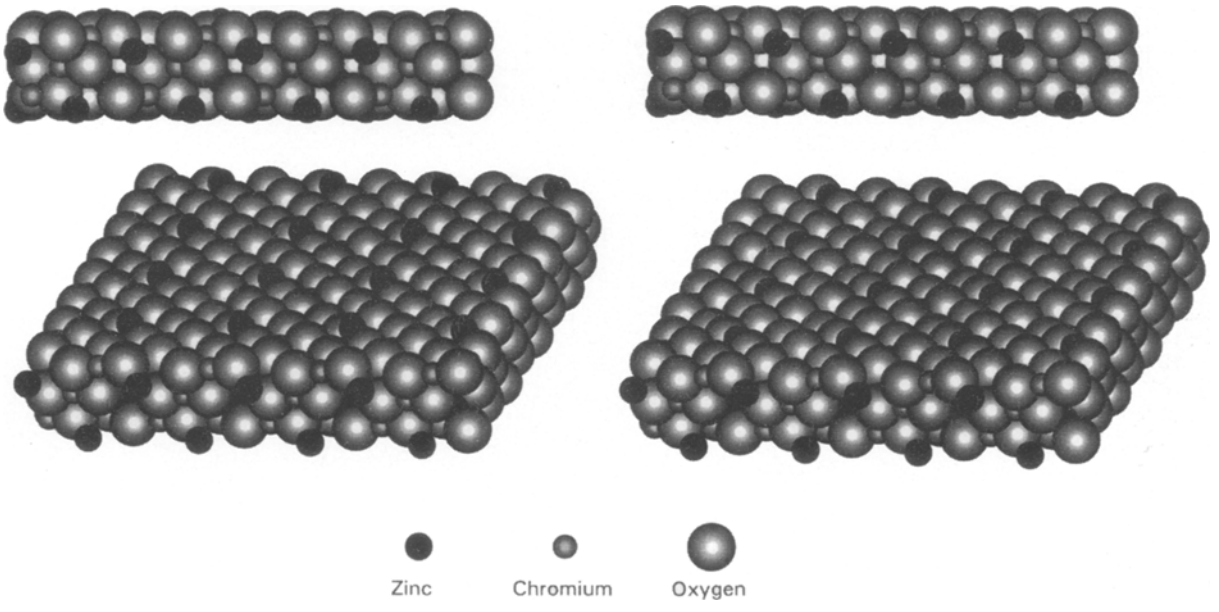

Figure 7 Atomic structure of a (4 0 0) surface stabilized by zinc interstitial ions.

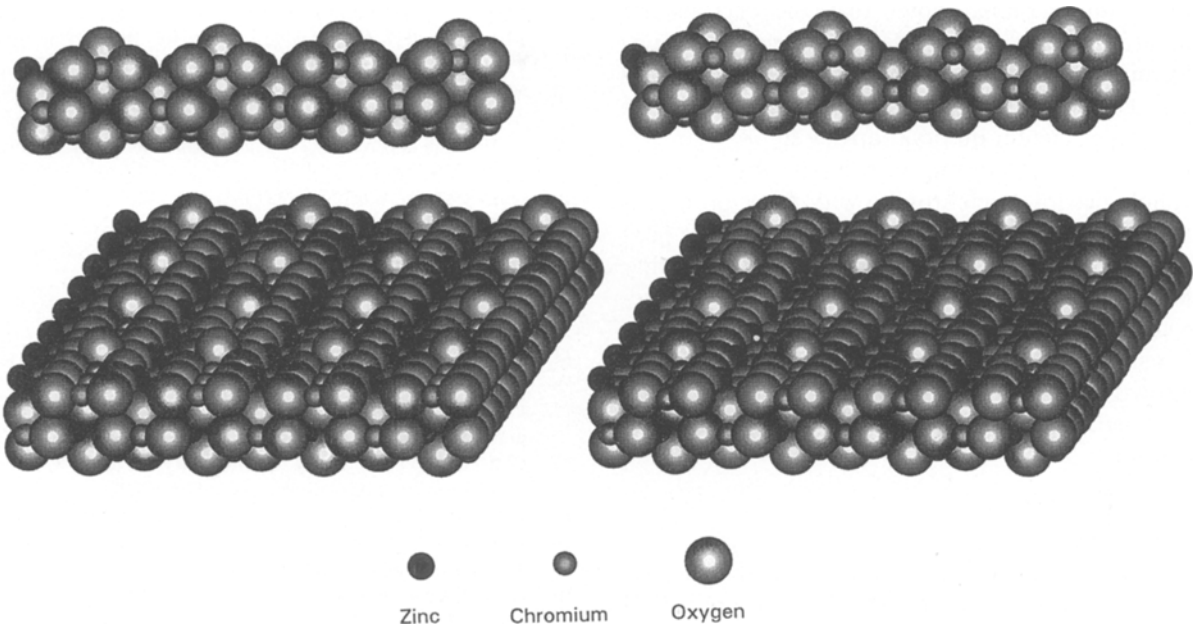

Figure 8 Atomic structure of a (2 2 0) surface stabilized by oxygen interstitial ions.

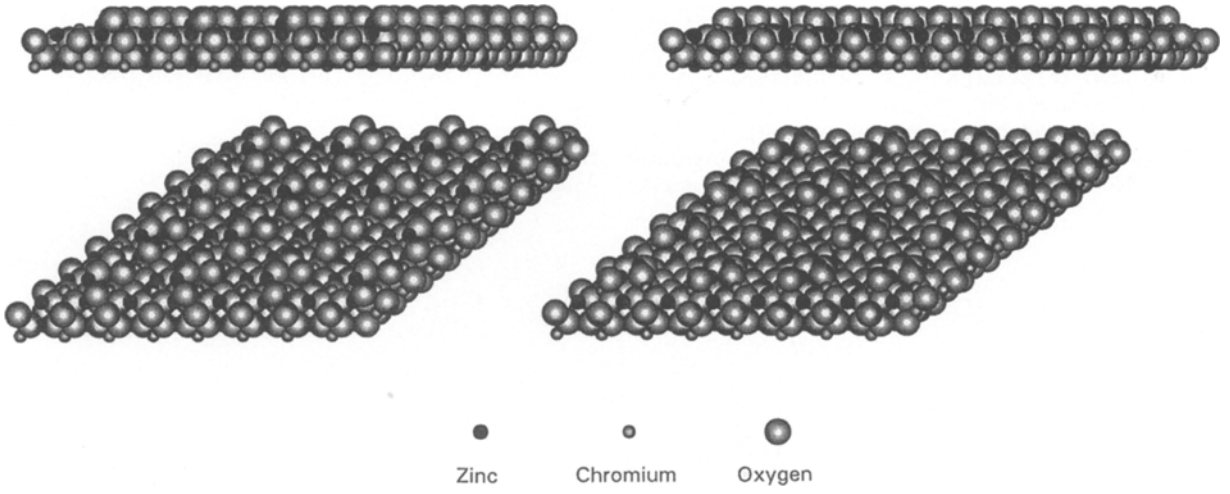

Figure 9 Atomic structure of a (1 1 1) surface stabilized by $(4O_i^{\parallel} + 3V_{Zn}^{\parallel})$.

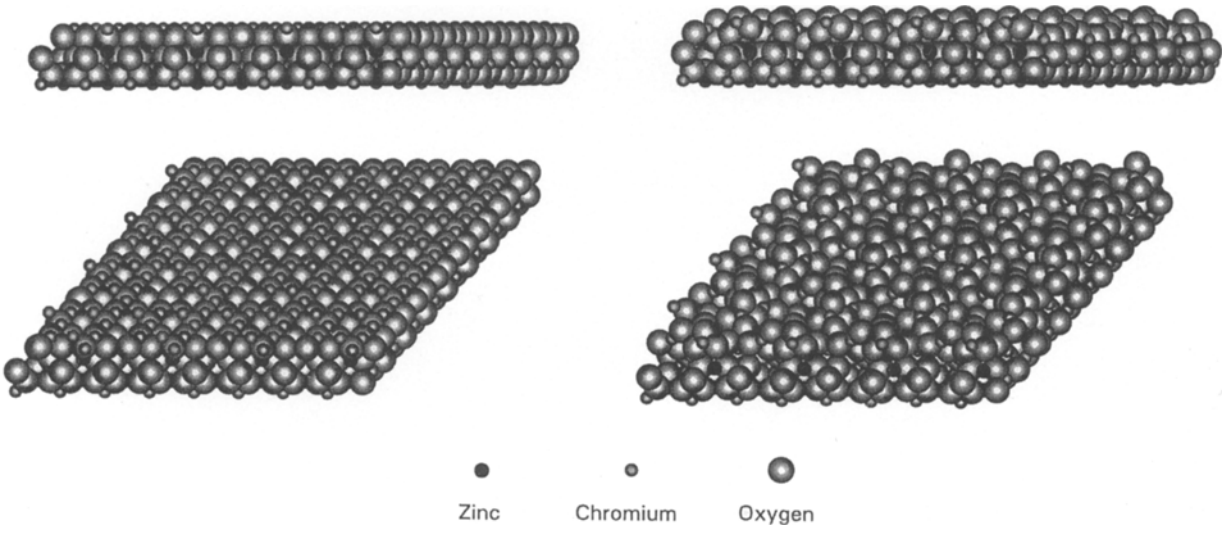

Figure 10 Atomic structure of a (1 1 1) surface stabilized by $(6V_{Zn}^{\parallel} + 4V_{Cr}^{\parallel\parallel})$.

reported micrographs shows that the crystals are dominated by the (1 1 1) surface. However, the non-uniformity of the reported crystallites does not allow us to be certain that the attachment energy model best fits the experimental observations.

It is therefore interesting to compare the predicted morphologies for zinc chromite with those found experimentally for the similar spinel zinc cobaltite [23] grown using chemical vapour techniques. The quality of these data is much better and clearly shows a structure largely dominated by the (1 1 1) surface together with a small degree of capping. As such it seems that the growth morphology is being reproduced, although more experiments are required for us to form a definite conclusion.

References

1. Y. SHIMIZU, S. KUSANO, H. KUWAYAMA, K. TANAKA and M. EGASHIRA *J. Am. Ceram. Soc.* **73** (1990) 818.
2. M. BERTOLDI, M. FUBINI, G. GIAMELLO, G. BUSCA, F. TRIFIRO and A. VACCARI, *J. Chem. Soc. Farad. Trans. I* **84** (1988) 1405.
3. A. RIVA, F. TRIFERO, A. VACCARI, L. MINTCHEV and G. BUSCA, *ibid.* **84** (1988) 1423.
4. E. GIAMELLO, B. FUBINI, M. BERTOLDI, G. BUSCA and A. VACCARI, *ibid.* **85** (1989) 237.
5. B. FUBINI, E. GIAMELLO, F. TRIFIRÒ and A. VACCARI, *Thermochim. Acta* **133** (1988) 155.
6. D. J. BINKS, PhD thesis, University of Surrey, and AEA-TPD-368, AEA Technology Harwell Report (1994) "Computational Modelling of Zinc Oxide and related Oxide Ceramics".
7. V. E. HENRICH and P. A. COX, in "The Surface Science of Metal Oxides" (Cambridge University Press, Cambridge, 1994).
8. M. J. DAVIES, S. C. PARKER and G. W. WATSON, *J. Mater. Chem.* **4** (1994) 813.
9. D. H. GAY and A. L. ROHL, *J. Chem. Soc. Farad. Trans.* **91** (1995) 925.
10. D. E. PARRY, *Surf. Sci.* **49** (1975) 433.
11. *Idem, ibid.* **54** (1975) 195.
12. D. J. BINKS and R. W. GRIMES, *J. Am. Ceram. Soc.* **76** (1993) 2370.
13. D. J. BINKS, R. W. GRIMES and A. B. LIDDIARD, *Philos. Mag.*, **72** (1995) 651.
14. B. G. DICK and A. W. OVERHAUSER, *Phys. Rev.* **112** (1958) 90.
15. C. R. A. CATLOW, W. C. MACKRODT, M. J. NORGETT and A. M. STONEHAM, *Philos. Mag.* **35** (1977) 177.
16. C. R. A. CATLOW and W. C. MACKRODT (eds), "Computer Simulation of Solids" (Springer, Berlin, 1982).
17. J. H. HARDING, *Rep. Prog. Phys.* **53** (1990) 1403.
18. C. R. A. CATLOW and A. M. STONEHAM, *J. Chem. Soc. Farad Trans.* **85**(5) (1989) Special Issue.
19. A. H. HARKER and R. W. GRIMES, *Mol. Sim.* **4** (5) (1990) Special Issue.
20. P. W. TASKER, *J. Phys. C Solid State Phys.* **12** (1979) 4977.
21. H. A. DABKOWSKA, *J. Cryst. Growth* **54** (1981) 607.
22. F. LECCABUE, C. PELOSI, E. AGOSTINELLI, V. FARES, D. FIORANI and E. PAPARAZZO, *ibid.* **79** (1986) 410.
23. W. PIERARCZYK, P. PESHEV, A TOSHEV and A. PAJACZKOWSKA, *Mater. Res. Bull.* **23** (1988) 1299.

Received 8 August
and accepted 8 September 1995